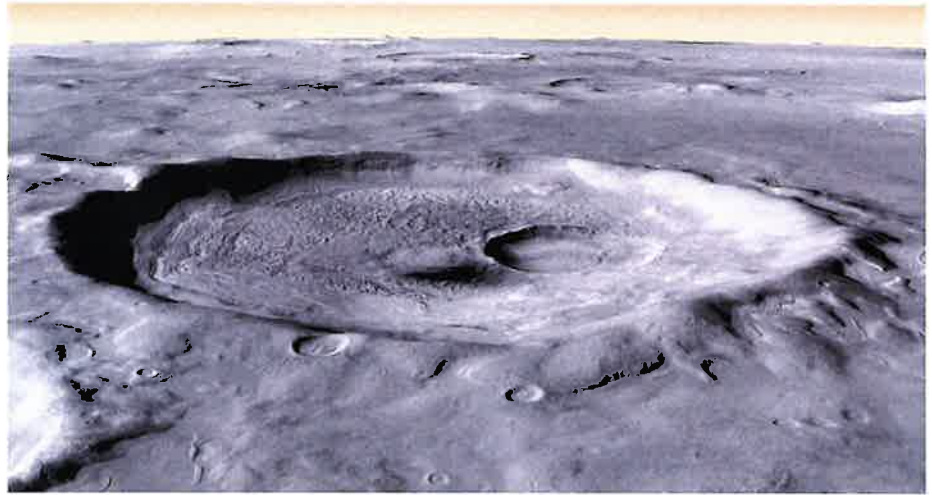# Potential glacial landforms in Nilosyrtis Mensae, Mars
- A qualitative geomorphological mapping and interpretation of an inpact crater

Aili Vesmes

Degree of Bachelor of Science
with a major in Earth Sciences
15 hec

Department of Earth Sciences
University of Gothenburg
2023 B-1265

UNIVERSITY OF GOTHENBURG

Faculty of Science

Potential glacial landforms
in Nilosyrtis Mensae, Mars
- A qualitative geomorphological mapping
and interpretation of an inpact crater

Aili Vesmes

Abstract

The surface of Mars is composed of a variety of geological formations, including mountains, volcanos, canyons, and plains. Studies of regions at mid-latitudes of the northern dichotomy boundary of Mars have demonstrated the presence of landforms that are morphologically analogous to glacial and periglacial landforms on Earth. Due to the cold and arid climate on the planet, glaciers on Mars are generally viewed as cold-based, rather than warm-based. Recent studies suggest, on the other hand, that warm-based glaciers may have existed locally for limited periods of time.

In this study a geomorphological map of an impact crater in an area called Nilosyrtis Mensae is produced. The aim of the thesis is to investigate which potentially glacial landforms occur in the study area, and investigate the possibility that a warm-based glacier has been present in the study area. To answer these questions, CTX- and HiRISE-images have been used to identify and map different landforms. Out of twelve identified landforms, several are interpreted to have a glacial or periglacial origin, including glacier-like formations (GLF), concentric crater fills (CCF) and thermal contraction polygons. In addition, observations of eroded crater walls and the degradation of a crater rim imply basal sliding and glacial abrasion may have occurred in the study area, which in turn suggests that a warm-based glacier may have existed. Further research is suggested for the understanding of the formation of a warm-based glacier in the study area since this is still unclear.

Table of Contents

1. Introduction

Mars, the red planet, has long amazed and fascinated humanity. Since the first images of the Martian surface were produced almost 50 years ago by NASA's Mariner 4 satellite, many advances have been made in the field (Forget et al., 2007). Today, several satellites and rovers have provided valuable data and information on the geological properties of the planet. Despite this, there are still many unexplored places on the surface of Mars.

Like on Earth, the surface of Mars has a complex geology, including mountains, volcanos, canyons and plains. The Martian landscape also show evidence of exogenous processes such as glacial and fluvial landforms, which were formed during a time when the planet had a denser atmosphere that could keep enough heat for liquid water to exist. Today, Mars is a tectonically rather inactive planet and has lost its protective magnetic field. The low atmospheric pressure on the planet causes liquid water to sublimate on the surface. Today, most of the water on Mars is contained as ice in the polar ice caps and as preserved glaciers in the high- to mid-latitudes. (Forget et al., 2007).

Glaciers can be distinguished into two types based on their internal thermal conditions, warm- or cold-based glaciers. Warm-based glaciers are glaciers where the glacial ice has reached its melting temperature during part or all of the year and form lenses and streams of liquid water at the base of the glacier. The water may originate from meltwater on the surface of the glacier, melting of ice at the base of the glacier due to trapping of heat rising from the ground or melting due to a lowering of the melting point of ice caused by a higher pressure by the weight of overlying ice. Movement in warm-based glaciers involves both internal plastic deformation and basal sliding, which occurs when water collects at the base of the glacier allowing it to glide along the bedrock. Cold-based glaciers, on the other hand, are glaciers where the glacial ice remain below melting temperature at the base throughout the year due to cold atmospheric temperatures. Movement in cold-based glaciers generally only occurs through internal plastic deformation. (Benn & Evans, 2014)

The general view has been that glaciers on Mars are cold-based, which would result in minimal glacial erosion and a lack of glacial landforms. However, recent observations and studies suggest that warm-based glaciers may have existed locally for limited periods of time. Landforms have been observed on Mars that resemble glacial landforms on Earth, such as eskers, streamlined formations and moraine-like ridges. (Butcher et al., 2017; Gallagher et al., 2021; Woodley et al. 2022)

Due to the difficulty of performing direct research on Mars, scientists often use analogous environments on Earth, such as Antarctica and Svalbard, to interpret landforms and their formation process. However, it is important to be careful when drawing parallels between two different planets, as the planetary conditions and dynamics can be significantly different. Landforms that look the same on Earth may have different origins on Mars. (Hauber et al., 2011)

1.1 Aim and Objectives

The objectives of the thesis are listed below:

- To complete a geomorphologic map of landforms in the study area.
- To evaluate which landforms are potentially glacial in origin in the study area.
- To evaluate the hypothesis that a warm-based glacier has been present in the study area.
- To contribute to a deeper understanding of Mars geological history in the region of the study area.

1.2 Study Area

This project will focus on an impact crater (coordinates 71.359719°E, 35.194952°N) in an area called Nilosyrtis Mensae (figure 1). The crater is about 30 km in diameter and has a younger impact crater (ca 8 km diameter) inside it where there currently lies a glacier-like formation showing flow features, likely made of ice rich-deposits. Nilosyrtis Mensae is an area where the northern lowlands meet the more dramatic southern highlands. Previous observations show that the area is characterized by ridges, valleys and gullies indicating erosion of a flowing material, probably from glacial and fluvial processes (Levy et al., 2007).
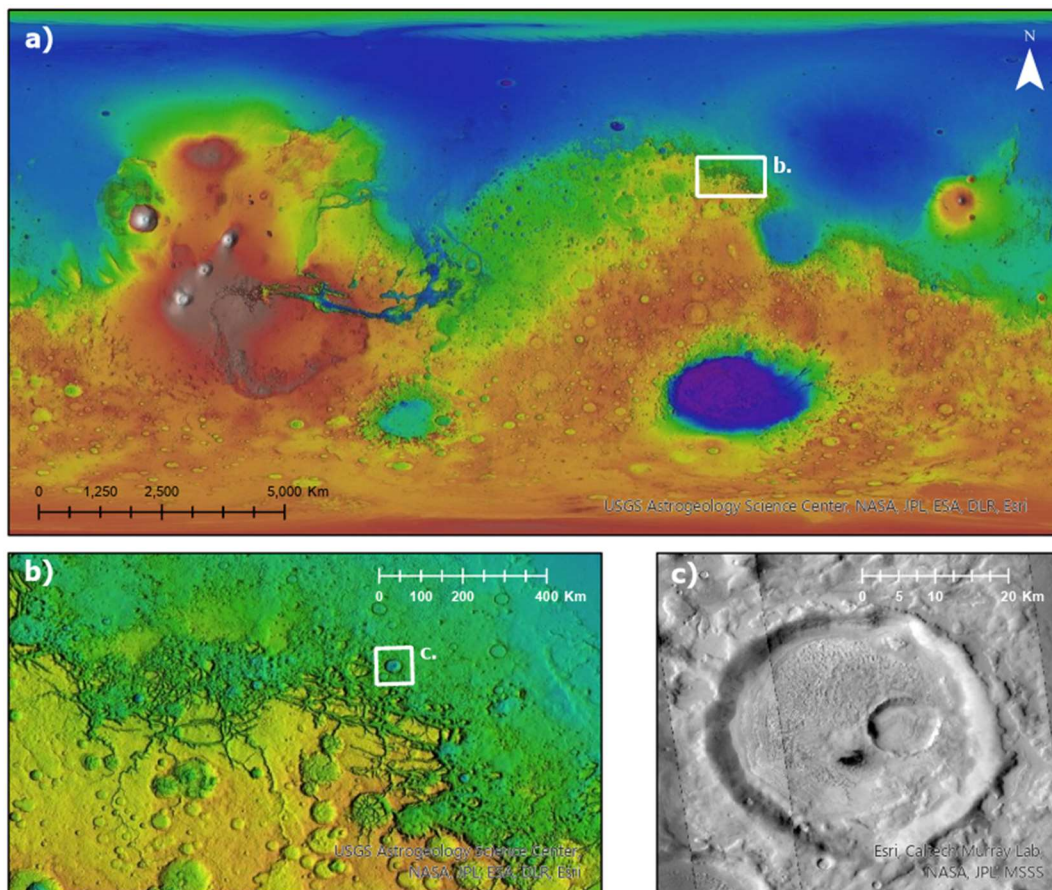

Figure 1. a) Global elevation map of Mars with Nilosyrtis Mensae marked by the white rectangle. b) Elevation map of Nilosyrtis Mensae, the studied impact crater is marked with the white rectangle. c) Merged CTX images of the studied crater. Image credit: NASA MGS/MOLA and NASA/JPL/MSSS

2. Background

2.1 Introduction to Mars

Mars is the fourth planet from our sun and located outside Earth's orbit. The planet has a mean diameter of 6779 km compared to Earth's 12742 km (Forget et al., 2007). The surface of Mars is about the same size as the combined land surface of Earths continents. The planet has an Earth-like structure, differentiated into crust, mantle and core. Since Mars is a smaller planet than Earth, it is believed that it cooled very rapidly and that today the core is most likely solid. Due to the lack of movement in the core the planet has lost its protective magnetic field, although paleo-magnetic remnants in the crust indicate that it was once there (Forget et al., 2007).

A notable feature of Mars topography is a distinctive topographic difference between the high southern hemisphere and the lower northern plains (figure 2). The average difference in altitude between the two areas is 5 km and the southern high plateau is heavily crated and considered old, while the surface of the northern plains is younger and has fewer craters in comparison (Forget et al., 2007). The crust in the southern hemisphere is much thicker compared to the north, which is, together with the fact that Mars show no plate-tectonic activity, believed to cause much greater topographic variations on Mars than on Earth (Forget et al., 2007). A transitional zone between the two areas unevenly circles the entire planet between 45°N and 10°S. The zone is characterized by highly eroded terrain, faults and isolated hills with steep sides and flat tops (Forget et al., 2007). The explanation of the dichotomy is still uncertain, but one hypothesis is that it was formed by an oblique impact during the very earliest stage of the Martian history, and is therefore possibly the oldest recorded geologic event on Mars (Carr & Head, 2010).
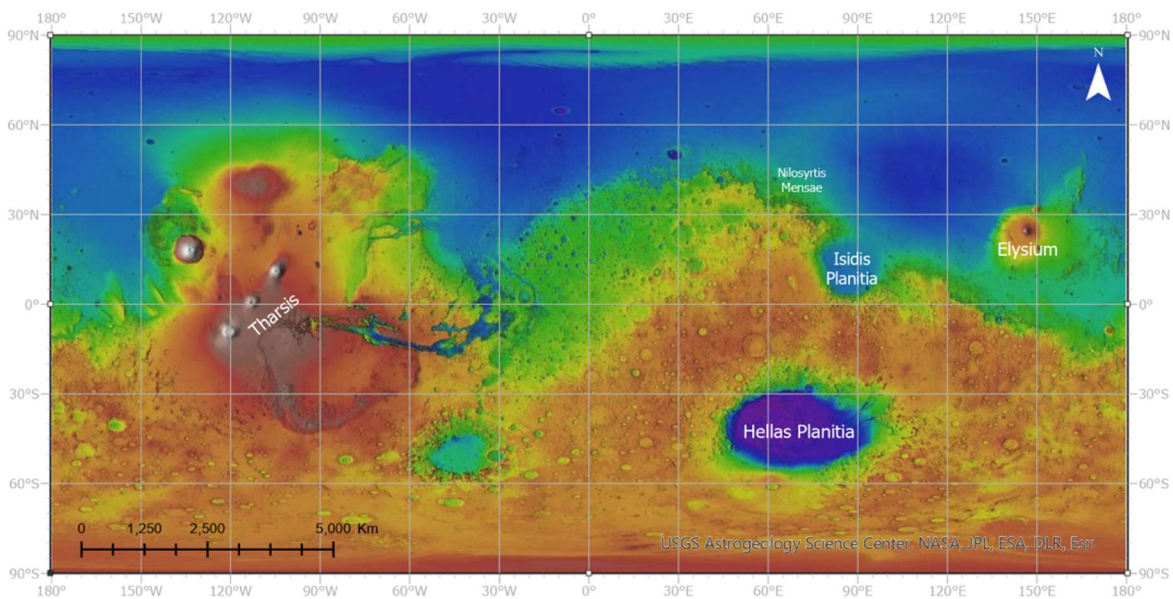

Figure 2. Global elevation map of Mars with main Martian landmarks. Note the topographic difference of the northern and southern hemispheres. Image credit: NASA MGS/MOLA

The lack of a magnetic field and the low gravity on Mars resulted in the formation of a thin atmosphere which is subjected to solar wind erosion (Forget et al., 2007). The atmosphere of Mars consists of 95.3% CO_2, 2.7% N, 1.6% Ar, 0.13% O and 0.03% water vapor compared to Earth's 0.035% CO_2, 78% N, 0.93% Ar, 20.6% O and approximately 0.4% water vapor (Forget et al., 2007). Noteworthy are the differences in amount of carbon dioxide, nitrogen and oxygen between the planets' atmospheres. Temperatures can vary during day and night between +20°C and -100°C, which is due to the thin atmosphere and the soil's inefficiency at storing heat, compared to the Earth's oceans (Forget et al., 2007).

2.2 Martian Geologic History

The geologic history of Mars is divided into four major time periods (figure 3). Without samples from Mars's surface, it is difficult to date the periods identified. Today scientist use a method based on counting craters to receive a relative age of a region on Mars, these calculations can then be calibrated to lunar rock samples to receive an absolute dating (Forget et al., 2007).

The oldest period is called pre-Noachian and extends from the time of the formation of the planet (ca. 4.5 Ga) to the formation of the Hellas basin (ca. 4.1 Ga). During this period Mars was heavily bombarded by impacts, most likely had a magnetic field, and the global dichotomy was formed at the beginning of this period. After pre-Noachian comes the Noachian period, which ranges from ca 4.1 Ga to ca. 3.7 Ga. This period is distinguished by high rates of cratering, erosion, valley formation and volcanism that affected the landscape. Furthermore, a significant amount of water probably accumulated on the surface of Mars during this period. The presence of hydrous weathering and the formation of valley networks and lakes suggests that Mars had, at least periodically, a warmer climate during the Noachian than today. The period following the Noachian is called the Hesperian, and extends from the end of heavy bombardments (ca. 3.7 Ga) to around 3 Ga. The Hesperian period is characterized by continued volcanism, low rates of erosion and valley formation compared to the Noachian, and formation of canyons, such as Valles Marineris, and large outflow channels. The current, and longest, period is the Amazonian which extends from ca. 3 Ga to present time. During the Amazonian changes to the surface due to impact cratering, volcanism and tectonism decreased and the pace of geologic activity slowed down. Consequently, the most distinctive characteristic of the Amazonian landscape are features connected to processes involving ice and wind. (Carr & Head, 2010)
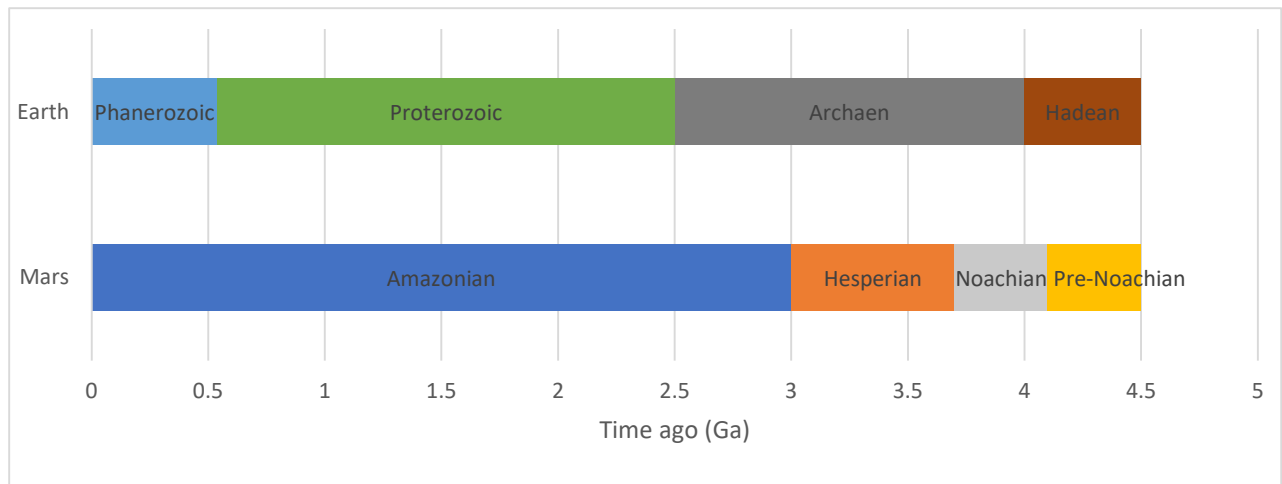
Figure 3. Geologic time periods of Mars compared to those of the Earth. Modified from Carr & Head (2010).

2.3 Glaciations on Mars

With a mean annual temperature of around -70°C, Mars has a permanently frozen surface. Despite this, the only visible stable ice masses are observed at the polar caps. Ice formed during the winter may be preserved on slopes with low solar radiation but will become unstable and sublimate as soon as spring arrives. The sublimation is possible because as the sun heats up the surface, the lowest part of the atmosphere is dried out and forces the ice to sublimate, even at negative temperatures. However, the sublimation can be prevented if the ice is isolated from the atmosphere by a layer of fine-grained sediments, making the ice stable even at lower latitudes. Evidence for the existence of sub-surface material rich in ice are lobate ejecta deposits around impact craters, which indicate that the collision with the frozen sub-surface has given rise to mudflow-like outflows. (Forget et al., 2007).

Like Earth, Mars experiences glacial and interglacial climate conditions. The variations of obliquity, meaning the tilt of the planet's polar axis, is believed to be an important factor for climate variations on Mars as it is on Earth. The obliquity of Mars is currently 25.2°, but it has undergone extreme variations from as little as 0° to as much as 60° throughout the planet's history. The reason for the large variations is that Mars does not have a large moon like Earth, but rather two much smaller moons, Phobos and Deimos, that are unable to stabilize the obliquity of the planet. (Forget et al., 2007; Laskar et al., 2004).

Interglacial conditions occur when the obliquity is low (between 0° and 20°). At these conditions, surface ice stability is driven poleward, preventing accumulation of ice and causing sublimation at lower latitudes (Madeleine et al., 2009). The seasonal variations are small and water and dust cycles are less active, causing a clear and dry atmosphere (Forget et al., 2007). At moderately high obliquity (between 25° and 40°) seasonal changes are more evident. The atmosphere becomes denser as CO_2 reservoirs are released and increases activity of the water and dust cycles (Forget et al., 2007). Midlatitude glaciations occur as vapor from ice deposits, held in the dust-rich atmosphere, precipitate at midlatitudes (Madeleine et al., 2009). At very high obliquity (between 40° and 60°) climate simulations suggest that polar ice

caps are almost entirely released into the dense, dust-rich atmosphere as water vapor (Forget et al., 2007). Formation of glaciers in the tropical latitudes might have been possible due to the large amount of water vapor in the atmosphere, that in turn could accumulate ice through condensation and precipitation (Forget et al., 2007).

In addition, observations have been made of features that appear to be formed of ice together with sediments, which show evidence for cyclical accumulation and loss of material as well as flow in their structure. One such feature is referred to as a 'Glacier-like formation' which consists of ice covered in boulders and other sediments exhibiting boulder-bands suggesting cyclical accumulation and sublimation of ice (Levy et al., 2021). Another feature is a several meter thick mantle consisting of a layer of ice and fine-grained sediment. This mantle is draped on older geological units, discontinuously distributed at latitudes 30°-60°, but continuously distributed towards the polar regions (Head et al., 2003). However, since the planet has different physical conditions compared to Earth, it is still unclear how glacier-like formations behave. It is suggested that ice on Mars must have a thickness of 1 km to be able to set a glacier-like formation in movement (Forget et al., 2007). A study done by Dickson et al. (2008) suggests that some glacier-like formations in the dichotomy boundary currently have a thickness of 1.5 km, but that the peak thickness of those glacial systems was possibly as much as 2.5 km.

2.4 Putative Glacial Landforms on Mars

Studies of regions at mid-latitudes of the northern dichotomy boundary of Mars have demonstrated the presence of landforms that are morphologically analogous to glacial and periglacial landforms on Earth.

2.4.1 Viscous Flow Features

Viscous flow feature (VFF) is a collective name for landforms that have surface morphologies associated with a viscous flow and is believed to be composed predominantly of ice. These landforms are located in Mars's midlatitudes and resemble terrestrial ice masses. The exact amount of ice in the formations is unclear since they are covered in a layer of fine-grained sediment. However, studies done with the shallow subsurface radar (SHARAD) sensor suggests that several VFFs possibly are composed of massive ice with minimal sediment content. VFFs are subdivided into three categories, Glacier-like forms, Lobate debris aprons and Lineated valley fills. Though these categories can vary in appearance, they have common characteristics such as lobate features, flow ridges, extension/compression ridges and surface lineation (figure 4). (Hubbard et al., 2014; Milliken et al., 2003)
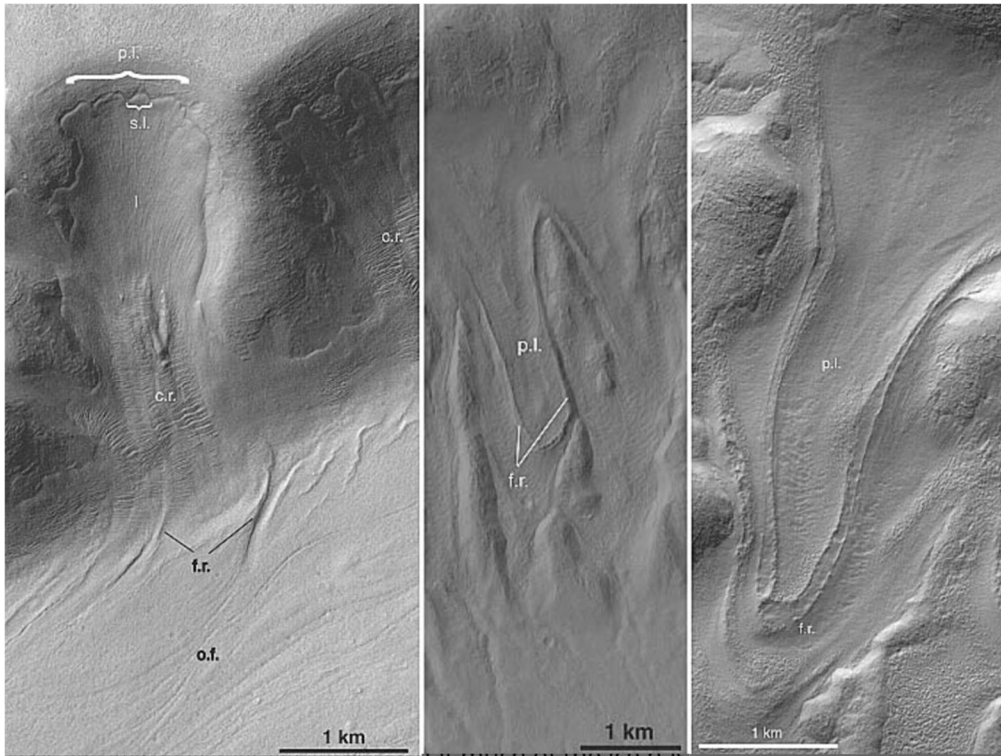
Figure 4. Examples of viscous flow feature characteristics, including primary lobes (p.l.), secondary lobes (s.l.), surface lineations (l), compression/extension ridges (c.r.), flow front ridges (f.r.), and older flow (o.f.). Modified from Milliken et al. (2003).

2.4.1.1 Glacier-like Forms

Glacier-like form (GLF) is a subcategory of VFFs that has a characteristic lobe-shaped tongue that resembles terrestrial valley glaciers. They generally originate from small alcoves or valleys and appear to flow downward between bounding sidewalls. GLFs usually terminates in a distinctive tongue shape at the base of a slope. (Hubbard et al., 2014)

2.4.1.2 Lobate Debris Aprons

Lobate debris aprons (LDA) often originate from merged GLFs that spread out at the base of a slope in a lobate nature (Hubbard et al., 2014). They are believed to be debris-covered glacier-like landforms, similar to rock-glaciers on Earth (Levy et al., 2021). The rocky debris on top of the glacier is believed to result partially from sublimation of ice that releases fine sediments trapped in the ice, and partially from transportation of large rocks (Levy et al., 2021).

2.4.1.3 Lineated Valley Fills

Lineated valley fills (LVF) are formed when LDAs and GLFs meet from opposite sides of a valley. They are characterized by complex and contorted surfaces without an obvious flow direction, but is commonly lineated along the axis of the valley. (Hubbard et al., 2014; Levy et al., 2007)

2.4.2 Concentric Crater Fills

Concentric crater fills (CCF) are similar in composition to VFFs, meaning they consist of a viscous flow believed to be composed of ice and sediments. The difference is that CCFs are always bound to a crater. The flow moves from the crater walls and fills the base of the crater (figure 5). CCFs are characterized by a sequence of concentric compressional ridges. In some areas, CCFs can become integrated into other viscous flow systems by completely filling the crater resulting in material spilling over into the surrounding area or through openings in the crater walls where an exchange of material can occur. CCFs are only found within the midlatitudes of Mars. (Dickson et al., 2012)
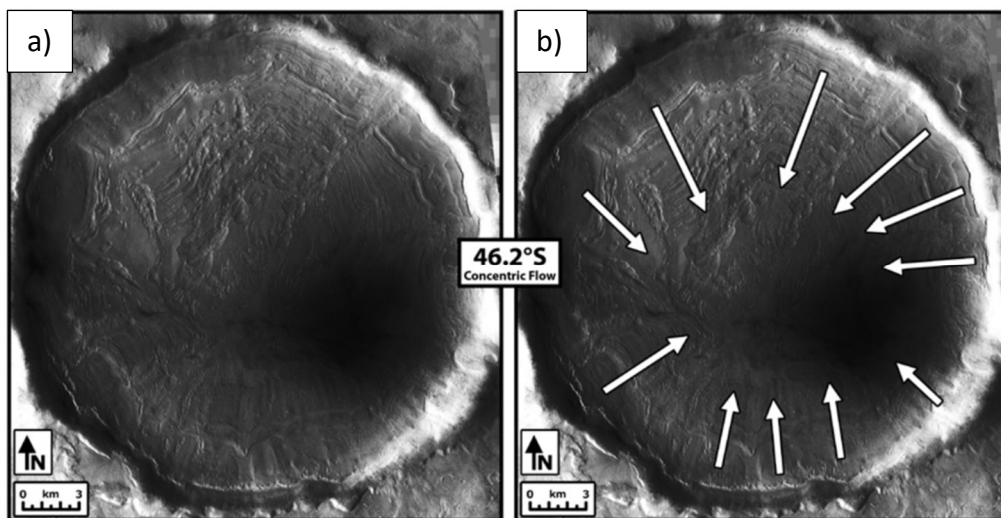

Figure 5. a) Concentric flow of ice in the southern mid-latitudes (46.2°) (subframe of CTX orbit P19_008308_2265). b) Interpretation of flow direction. Figure from Dickson et al. (2012).

2.4.3 Scalloped Depressions

Scalloped depressions are interpreted to be periglacial landforms and are thought to be the result of ground-ice degradation. These depressions usually have a circular to elliptical shape and can range between tens of meters to several kilometers in diameter with depths up to ten meters (figure 6a). Similar depressions on Earth are strongly associated with thaw processes, but it is still unclear how the depressions form on Mars. However, the suggestions are either a formation based on thawing of ground-ice followed by evaporation or sublimation of ground-ice followed by removal of the remaining lag by eolian processes. (Séjourne et al., 2011)
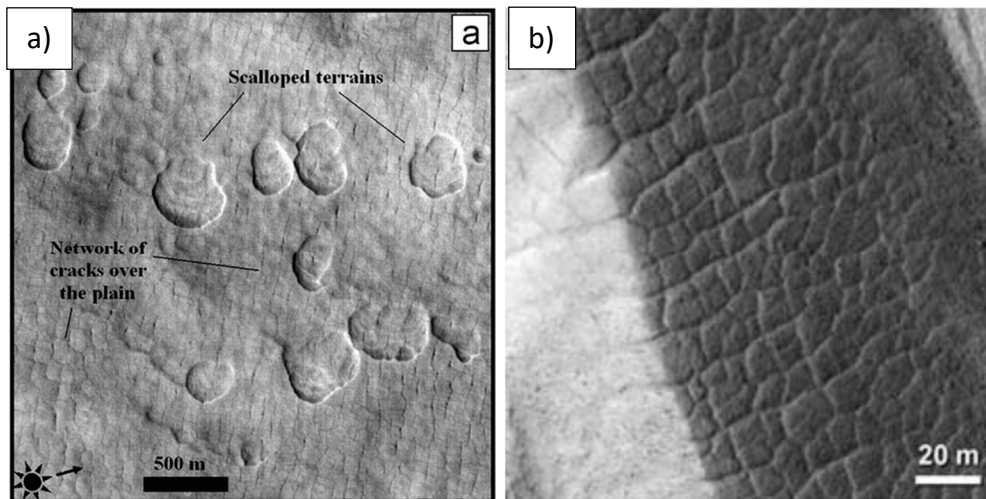
Figure 6. Example of a) scalloped depressions (Séjourne et al., 2011) and b) polygons pattern (Hauber et al., 2011) on Mars.

2.4.4 Thermal Contraction Polygons

Cold climate polygons are widespread both on Earth and Mars. The pattern is formed by thermal contraction cracks (figure 6b), driven by annual temperature changes, and suggest that ice is present just a few centimeters below the overlaying sediments. When cracks occur on the surface, finer material are gathered in them leaving coarser material at the surface, which in turn makes the ground more sensitive to sublimation. (Forget et al., 2007; Marchant & Head, 2007).

3. Method

3.1 Data Handling

Data that has been used for the geomorphological mapping and observations consists of satellite images taken with the Context Camera (CTX) and the High Resolution Imaging Experiment (HiRISE) camera equipped on Mars Reconnaissance Orbiter (MRO).

The images have been downloaded from the PDS Geosciences Node Mars Orbital Data Explorer (ODE), a database over satellite data from several Mars missions, together with corresponding label and header files. In addition, a digital elevation model (DEM) was provided from MARS Système d'Information (Mars-SI). All data used in the project is listed in table 1.

Table 1. Information about the used datasets.

Datasets	Resolution and file type	Satellite /Camera	Source
B19_017063_2155_XI_35N288W	5 m/pixel pyramidizied GeoTIFF ISIS Header	MRO CTX	Mars Orbital Data Explorer
B19_016852_2156_XN_35N289W	5 m/pixel pyramidizied GeoTIFF ISIS Header	MRO CTX	Mars Orbital Data Explorer
B18_016641_2137_XN_33N288W	5 m/pixel pyramidizied GeoTIFF ISIS Header	MRO CTX	Mars Orbital Data Explorer
ESP_017063_2155_RED	25 cm/pixel .jp2 .lbl	MRO HiRISE	Mars Orbital Data Explorer
ESP_018276_2155_RED	25 cm/pixel .jp2 .lbl	MRO HiRISE	Mars Orbital Data Explorer
Mars CTX V01	5m/pixel	MRO CTX	The Bruce Murray Laboratory for Planetary Visualization
CTX_016641_2137_017063_2155-ALIGN-DEM	DEM .tif		Mars-SI

3.1.1 CTX-data

The CTX camera provides high resolution images of the surface of Mars and has been in orbit around the planet for 10 years. The resolution of the used CTX-files is 5 m per pixel and they have been used for observation and mapping of landforms in the study area. The Bruce Murray Laboratory for Planetary Visualization at the California Institute of Technology provides a global seamless mosaic over Mars' surface made from CTX images with a

resolution of 5 m per pixel. The mosaic was directly added to ArcMap through ArcGIS Online and has been used for overall observations of landforms in the study area and areas close by.

3.1.2 HiRISE-data

The HiRISE camera provides images of Mars surface with a very high resolution, 0.25 m per pixel. Images from HiRISE have been used for detailed observations of landforms and structures in the terrain. The availability of HiRISE images is limited and only a part of the study area was covered (figure 7).

3.2 Geomorphological Mapping

The geomorphological mapping has been made in ESRI ArcMap, version 10.9. A shapefile was created for every type of landform. The shapefiles have in turn been composed of either polygons or lines made with ArcMap Editor toolbar. When the mapping was done the map was exported from ArcMap as a PNG-file.

3.3 Elevation analysis

In addition to the geomorphological mapping, an elevation map was produced of the DEM provided from MarsSI. The DEM did not cover the whole study area, but a majority of the studied crater was included (figure 7). A hillshade layer and three elevation profiles was created from the DEM. The hillshade layer was made by the Hillshade tool in the ArcMap Spatial Analyst toolbox and the elevation profiles was made with the ArcMap 3D Analyst toolbar.
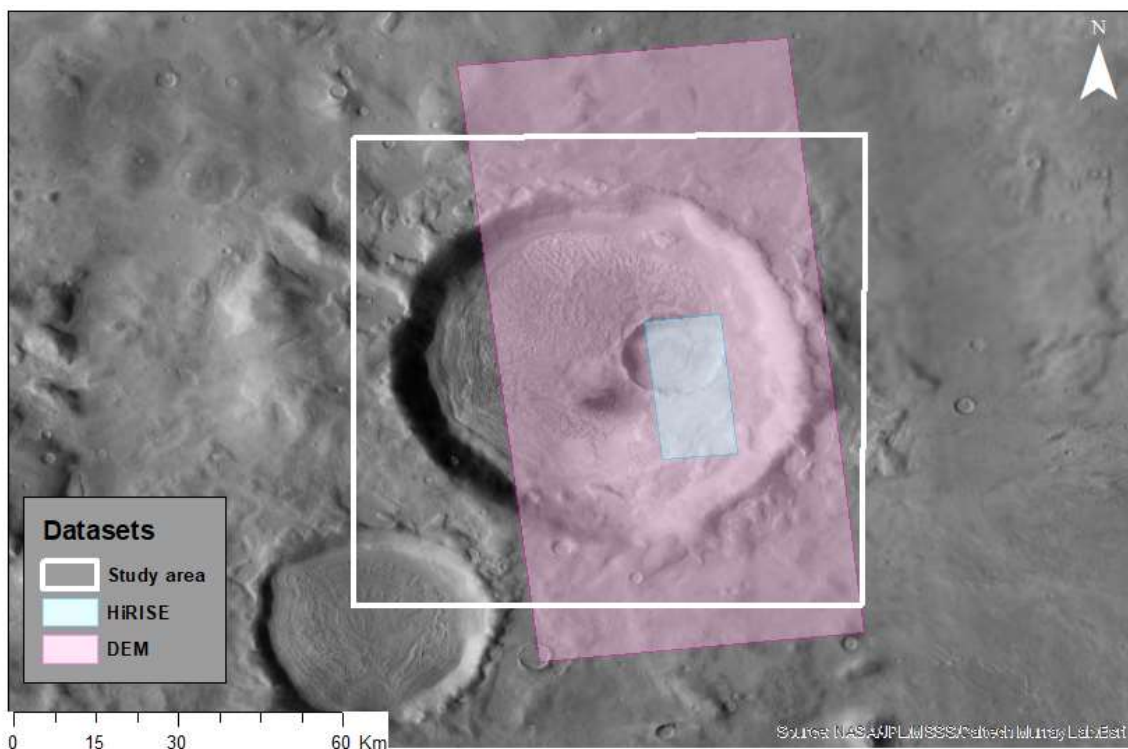

Figure 7. Map of the study area and the coverage of the HiRISE-data and DEM-data. Base map: CTX mosaic V01

4. Results

4.1 Geomorphological Map

Through the geomorphological mapping twelve landforms have been identified and mapped. The final map is represented in figure 8 and the observed landforms are further explained in *4.2 Observed Landforms*.
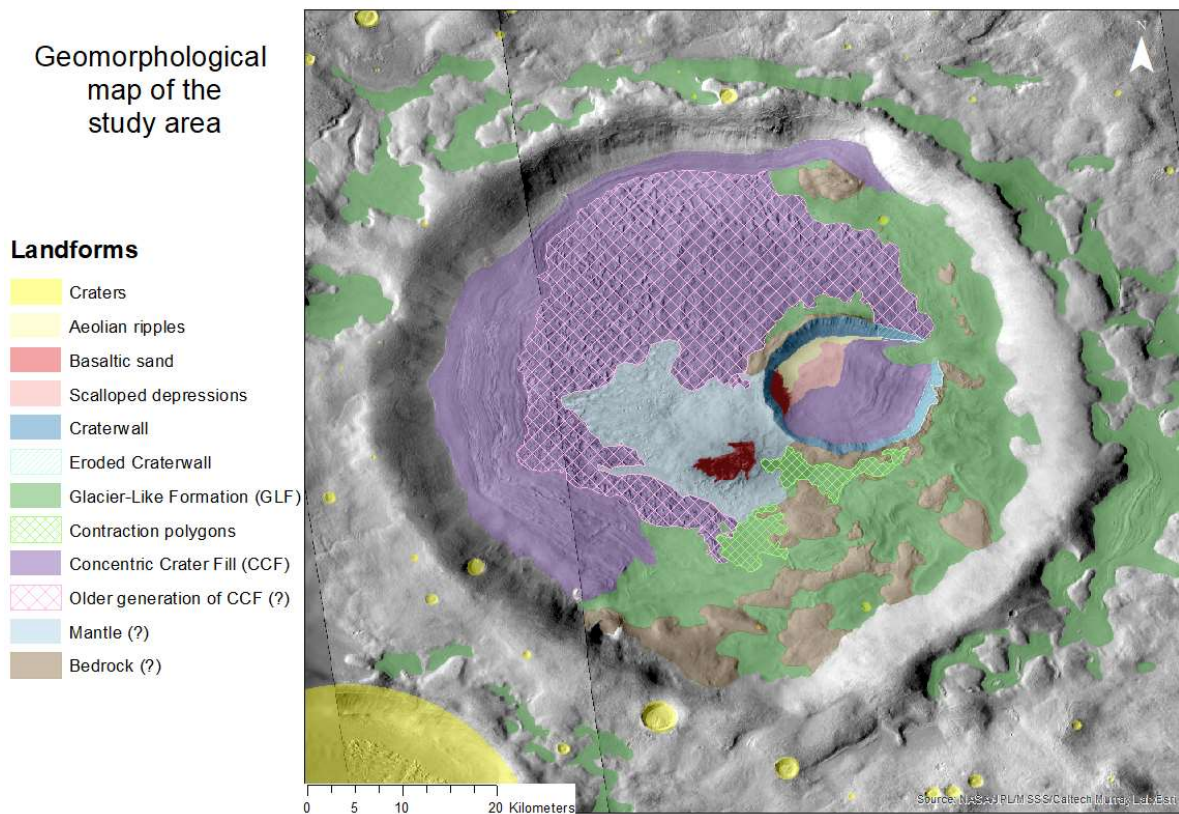

Figure 8. Geomorphological map of the study area. Sun direction from the left. Base map: CTX mosaic V01.

4.2 Observed Landforms

Four of the observed landforms have a direct connection with the presence of ice-rich deposits. These landforms are *Concentric crater fill* (CCF), *Glacier-like formation* (GLF), *Scalloped depressions* and *Thermal contraction polygons* on the surface. The CCF is distributed in the western part of the big crater, mainly expanding from the crater wall, and in the smaller crater, almost entirely covering the floor of the crater except for a section in the northeastern part. The CCF in both craters exhibit the characteristing compressional ridges. Cracks in the CCF are observed alongside the eroded crater wall in the small crater. That is the only place in the study area where cracks like these are discovered. The cracks seem to appear where the CCF meets the rocky crater wall. In the eastern part of the big crater a unit with a viscous flow was observed and interpreted as an GLF. The viscous flow is evident when observing ridges in the flow that exhibit a wavy structure and that the area seems smoothed. Areas with a similar smoothed appearance are also observed around the crater rim of the big crater. In the eastern part of the small crater the GLF seems to flow down creating a

lobate formed tongue into the small crater (figure 9). On the surface of the tongue, boulder bands with clustering boulders are observed. In two areas of the GLF, thermal contraction polygons (figure 10a) are discovered, indicating that the overlaying sediment layer is thin at these places. The scalloped depressions are found in the northwestern part of the small crater (figure 10b). The depressions vary in size from 10 m up to 50 m and are distributed in a 18.75 km^2 field. In addition, signs of sublimation is found in two other places in the study area, one just north of the small crater and the other outside the eastern parts of the big crater. At these two places the sublimation is exhibited in a line, similar to a pearl necklace, rather than a field (figure 10c).
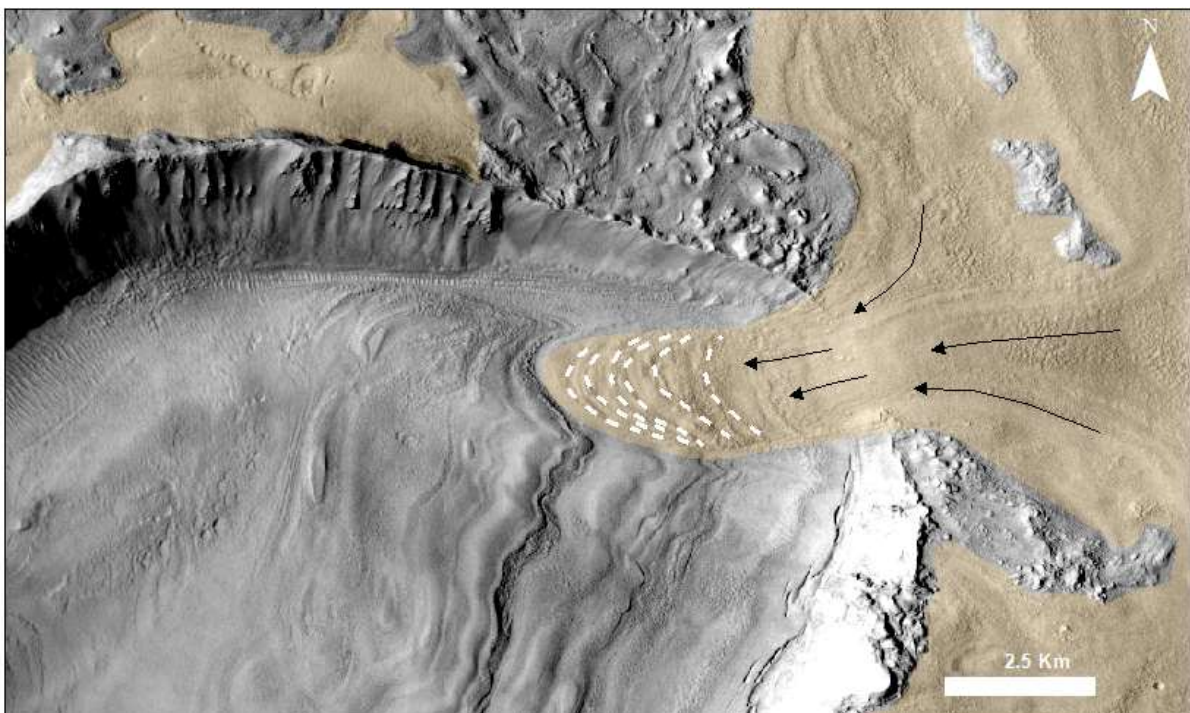
Figure 9. Glacier-like formation (GLF) flowing down into the small crater. Interpreted flow direction of the GLF is marked with arrows and repeated boulder bands are marked with dotted lines. Crevasse-like cracks alongside the eroded craterwall is visible south of the GLF. Image credit: NASA/JPL/MSSS

Observed landforms not directly connected to the presence of ice-rich deposits consists of *Craters*, *Basaltic sand*, *Aeolian ripples* and *Eroded crater walls*. A few smaller impact craters have been discovered in the study area, most of them outside the rim of the big crater but four were found inside the big crater and none in the smaller crater. Basaltic sand (figure 10e) is located in two places, one field in the center of the big crater and one field at the western crater wall of the small crater. Aeolian ripples of fine-grained sediment (figure 10d) were found in the northwestern part of the small crater. The basaltic sand and aeolian ripples made it hard to distinguish other landforms possibly hidden under the sediment. The eastern interior crater wall of the small crater differs from the rest of the crater walls. The surface of the crater wall seems smoothed and polished in comparison with the other parts that exhibit cliffs and a more structured surface (figure 11). Therefore, the eastern crater wall is interpreted as a

surface with more vigorous erosion than the rest of the crater walls. The extent of the more eroded crater wall is 21 km and are cut off by the GLF flowing down into the small crater.
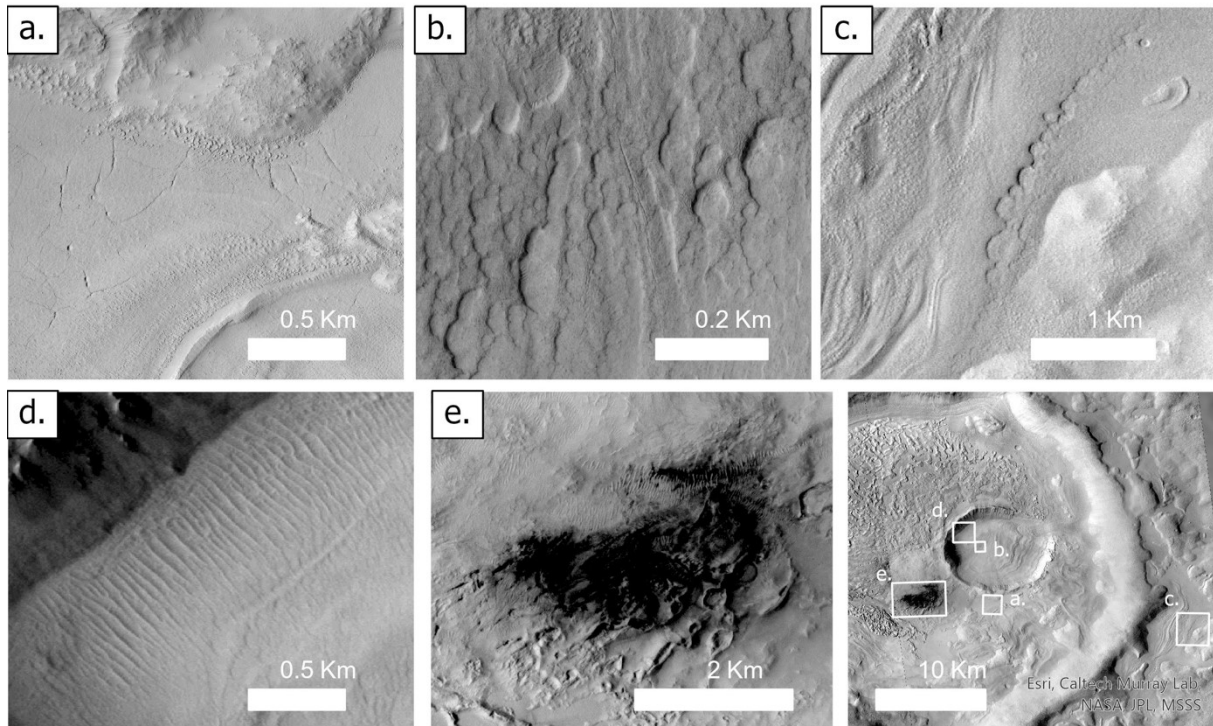

Figure 10. Interior and exterior landforms of the main crater. a) Thermal contraction polygons, b) scalloped depressions, c) sublimation depressions exhibited in a line, similar to a pearl necklace, d) aeolian sand ripples and e) basaltic sand. Image credit: NASA/JPL/MSSS
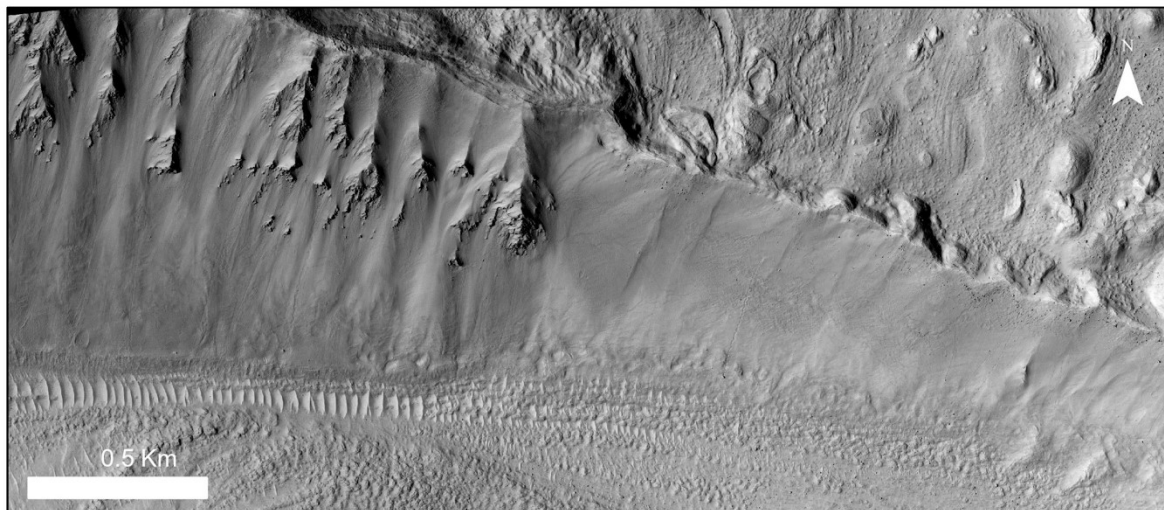

Figure 11. The northern interior crater wall. Note that slope spurs are preserved on the western part but are smoothed out on the eastern part. Image credit: NASA/JPL/MSSS

Lastly, three units were not as clearly identified and are therefore marked with question marks. These are *Mantle (?)*, *Older generation of CCF (?)*, and *Bedrock (?)*. The landforms that have been marked as *Bedrock (?)* has been interpreted as bedrock since the GLF seems to

flow around them, which indicate they have a higher elevation and are more resilient than surrounding areas. But it is unclear if the bedrock is coated with a layer of dust as the rest of the landforms or not, and in some places, it was hard to distinguish the bedrock. The exposed bedrock is mainly distributed in the southern parts of the big crater, but also occurs in the northwestern parts of the crater. In the center of the big crater a unit named *Mantle (?)* occurs. This unit has a relatively undisturbed surface, but it is unclear if the unit is connected to ice-rich deposits or not. The surface of this unit is flat, and the area seems covered in dust and sediments. Ripples of a fine-grained sediment are unevenly distributed in the area. The unit called *Older generation of CCF (?)* is one of the largest units in the study area. This area seems to consist of two intertwining units, one consisting of ridges in different directions and the other consisting of a smooth infilling in between the ridges (figure 12). The smooth infilling seems to be connected to the CCF and GLF surrounding the unit and could be interpreted as younger than the ridges. The ridges show signs of different stages of degradation, which could indicate that they consist of ice-rich deposits that have been exposed to surface conditions. The ridges could be material from an older CCF, formed by internal deformation and bulging.
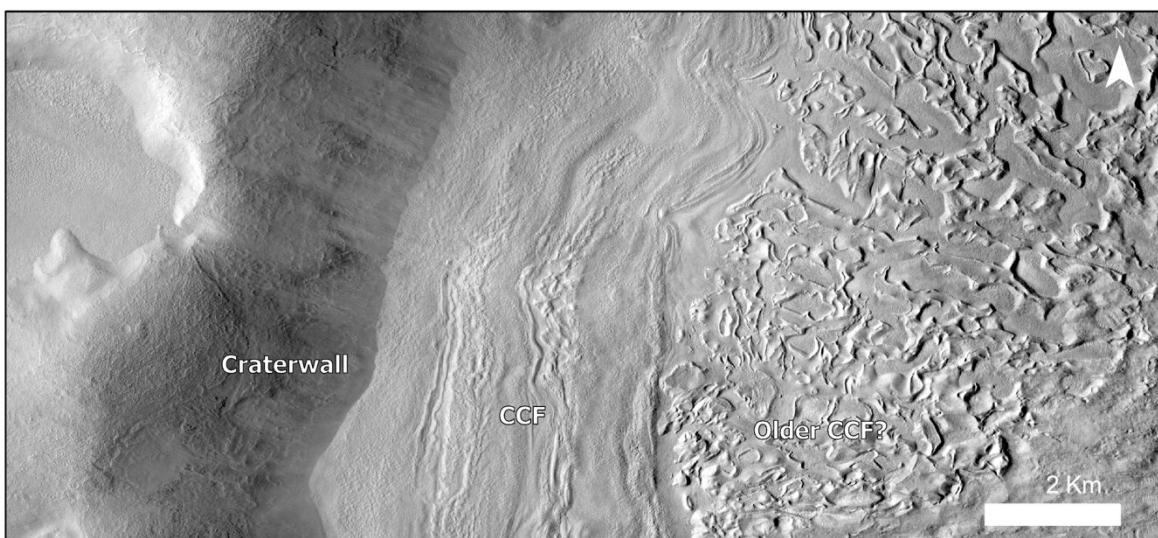

Figure 12. Transition from the craterwall, to CCF, and finally to a unit with a smooth infilling connected to the CCF intertwined with ridges that could be remnants from an older generation of CCF. Image credit: NASA/JPL/MSSS

4.3 Elevation Analysis

The elevation of the study area is represented in the elevation map in figure 13b. The highest elevation is at the crater rim, and the floor of the smaller crater represent the deepest surface in the study area. The northern crater rim exhibits a steeper crater wall than the southern and eastern crater rims, visualized by a faster transition from red to blue colors in the map.
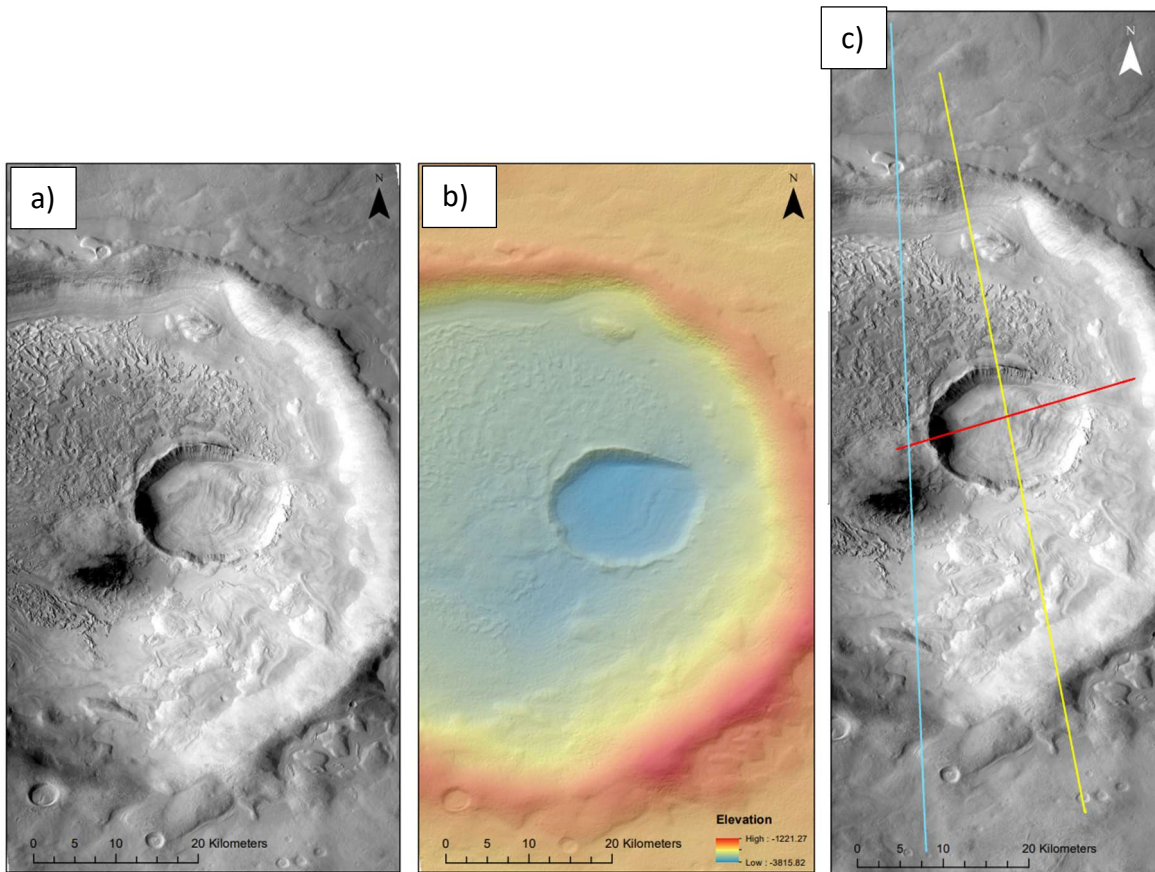
Figure 13. a) CTX images of the area with elevation data. b) Elevation map of the studied crater (hillshade + DEM). c) CTX images with three different elevation profiles marked blue, yellow and red. Image credit: NASA/JPL/MSSS

The blue elevation profile (figure 14) runs through the big crater from north to south. The crater rims are clearly visible as peaks and are characterized with steep crater walls into the crater. The southern crater wall rises in two stages compared to the northern wall which rises in a steep angel. The surface of the crater leans slightly towards the south. A similar representation is shown in the yellow elevation profile (figure 15), with the addition of the smaller crater in the middle of the profile. Another distinction between the yellow and blue profile is the elevation difference of the norther and southern crater rim. In the yellow profile the southern peak is ca 600 m higher than the northern peak, compared to the blue profile where the southern peak is ca 150 m higher than the northern peak. This is also visualized in figure 10b as the southwestern crater rim have a deeper red color, indicating it has a higher elevation, than the rest of the crater rim. The red elevation profile (figure 16) runs through the small crater from southwest to northeast. The southwestern crater rim is visible as a peak, while the northwestern crater rim is not as evident as the southwestern and seems degraded. Another difference is that the northeastern side of the crater rises continuously while the southwestern side have a clear steep slope.
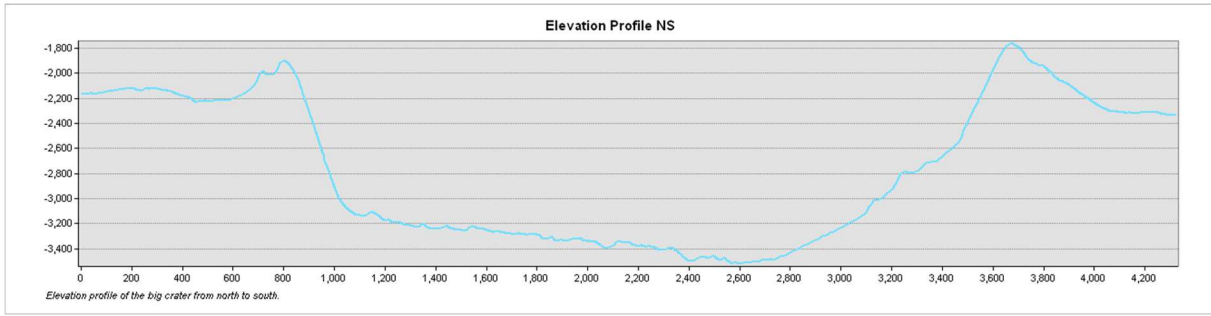
Figure 14. Elevation profile of the big crater from north to south. Note that the crater has a preserved morphology in terms of the rim.
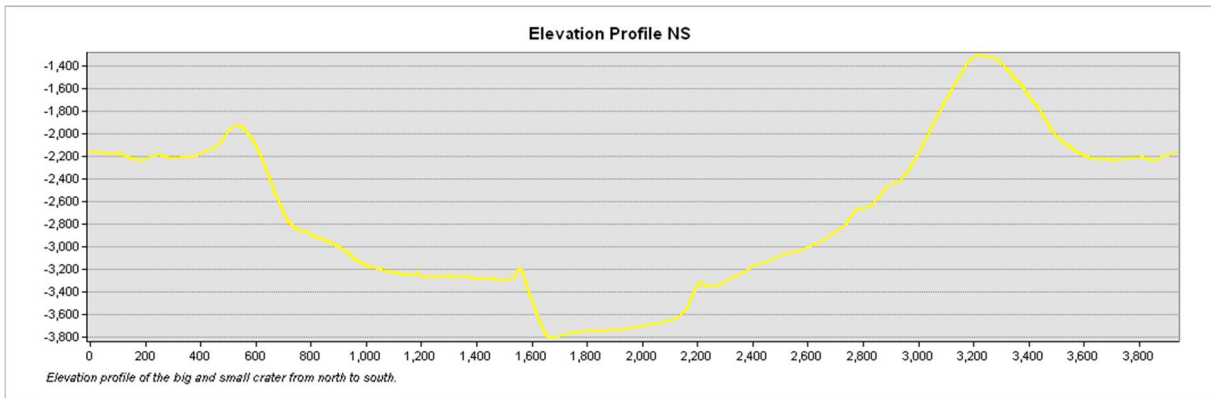

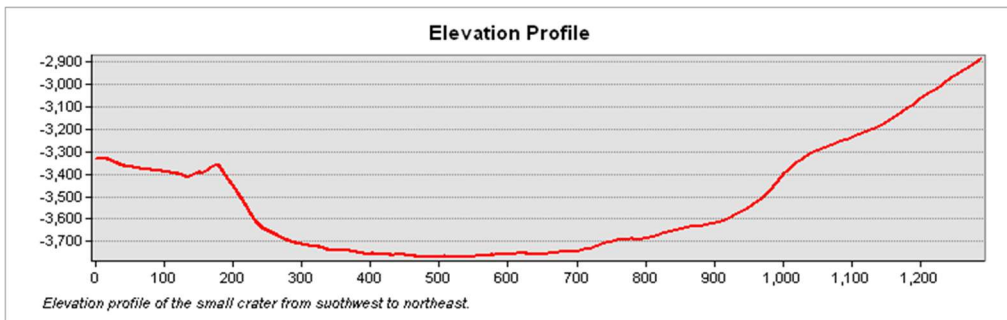**Figure 15.** Elevation profile of the big and small crater from north to south.

Figure 16. Elevation profile of the small crater from southwest to northeast. Note the smoothing of the crater morphology in the eastward direction.

5. Discussion

5.1 Observed Landforms

As the results reveal, several landforms with a potentially glacial origin were identified in the study area. This corresponds well with the view that more extensive glaciations are likely to have covered regions along the dichotomic boundary made by Levy et al. (2007) and Dickson et al. (2008). It is likely that the observed glacial and periglacial landforms were formed during different climatic episodes of glaciation during the history of Mars, and mainly those associated with the late Amazonian period. Only a few impact craters were discovered in the study area indicating that the surface of the area have been formed relatively recently.

Throughout the mapping it has been clear that there is a difference between the eastern and western parts of both craters. In the big crater, the difference mostly consists of the distribution between the *Glacier-like form* (GLF) in the eastern parts and the *Concentric Crater Fill* (CCF) in the western parts, where the GLF indicates a more active glacial area while the CCF seems relatively undisturbed. The formation of thermal contraction polygons in the southeastern parts of the crater indicate the presence of ice-rich deposits near the surface.

For the small crater, the eastern parts also show indications for more glacial activity. The most evident landforms are the GLF flowing into the crater from northeast and the erosion of the eastern crater walls. The red elevation profile (figure 16) reveals that the eastern crater rim is degraded, and that the elevation rises gradually, indicating a thicker layer of ice-rich depositions in the eastern parts of the crater. Another notable aspect is the shape of the crater, which does not exhibit the round bowl-shape of a characteristic impact crater. Instead, the eastern side of the crater appears to be excavated, creating an oval shape. The western part of the small crater contains a rather big area where sublimation scallops are present, which could indicate that this part of the crater have been more exposed to sunlight resulting in a higher amount of sublimation than the rest.

5.2 Possible Evolution of Glaciations

The whole study area shows signs of the presence of ice-rich deposits and glacial activity. Outside the rim of the big crater, formations with plateaus can be found in smaller impact craters and close to GLFs, indicating glacial ice have retreated in steps. In the big crater, the GLF, CCF and *Older generation of CCF (?)* implies that most of the crater once was covered with glacial ice. During a warmer period, the ice retreated revealing the ridges that are believed to represent the older generation of CCF. The age of the small crater is hard to establish, and it is unclear if it appeared before or after the ice retreated. Either way, the glacier has then advanced once more overlying landforms and flowing down into the smaller crater. The implications of glacial erosion, a thicker layer of ice-rich deposition and the shape of the crater suggests the glacier advanced from the east. As of today, this glacier has also retreated, uncovering the eroded crater walls.

5.3 The Possibility for a Warm-based Glacier

Of the observed landforms, two suggest the presence of a warm-based glacier, the eroded craterwall and boulder bands on the GLF. Cutting through the eroded crater wall, the tongue shaped GLF flows down into the small crater. The boulder bands, consisting of clustering boulders and fine-grained sediment, on the GLF resembles boulder bands on LDAs described by Levy et al. (2021), suggesting cyclical accumulation and sublimation of ice. The eroded crater wall suggest that erosion have been present alongside the eastern crater wall of the small crater. The smoothed and polished surface of the eroded crater wall and the degradation of the eastern crater rim may indicate basal sliding and glacial abrasion, that characterizes warm-based glaciers. These surface conditions were not observed on the other crater walls, suggesting the potential warm-based glacier was restricted to the eastern parts.

A requirement for the existence of warm-based glaciers is something that cause the glacial ice to melt either at the base, like heat rising from the ground, or on the surface, like atmospheric temperature (Benn & Evans, 2014). Since liquid water sublimates at the surface of Mars today (Forget et al., 2007), the melt of the ice needs to either have taken place at a time when Mars had a denser atmosphere or occur at the base of the glacier for the liquid water to be preserved. The surface of the study area is interpreted as relatively young due to the observation of few impact craters, which leaves melt at the base of the glacier as the most likely alternative for the existence of a warm-based glacier in the study area.

The recent studies suggesting the existence of local warm-based glaciers on Mars have been focused on observations in Phlegra Montes and Tempe Terra (Butcher et al., 2017; Gallagher et al., 2021; Woodley et al. 2022), sites relatively close to volcanic activity. The geothermal heat from volcanic activity is theorized to be the cause of the melting of glacial ice at the base of the glaciers. During this study no volcanic activity have been observed in or near the study area and it is therefore considered unlikely that a warm-based glacier with melting due to geothermal heat from volcanic activity have occurred. Another theory for melt of glacial ice at the base is the heat induced by an impact. It could be possible that the impact from the smaller crater produced enough heat to transform the ice-rich deposits in the eastern parts of the big crater into a warm-based glacier. The age of the small crater has not been established and it is therefore difficult to determine if the impact was made recently enough to have an influence on the ice-rich deposits currently in the study area. Further investigations of the thermal environment and age of the craters could help to get a better understanding of the study area and the possibility of a warm-based glacier.

5.4 Limitations and Difficulties

The study of geomorphology on a different planet comes with both difficulties and limitations since remote sensing is the only option for research. Though today's technical evolution provides data of various types and resolutions, field observations, samples and tests are needed to fully establish the origin of landforms. Until that is possible, the use of analogous environments on Earth and the knowledge that planetary conditions and dynamics can be

significantly different are a planetologists best tools to interpret landforms and their formation process on different planets.

Besides the lack of direct research, the main limitation of this study has been the limited coverage of high-resolution images, such as HiRISE images, of the study area. This have affected the detailed observations of landforms in the study area and made detailed mapping more challenging. Furthermore, the mapping could be subjective and mistakes in the interpretations may occur that could influence the results.

6. Conclusions

The main objectives of this thesis were to produce a geomorphologic map and investigate which potentially glacial landforms occur in the study area. Through the mapping, twelve different landforms have been identified and mapped in the study area. Seven of those are interpreted to have a glacial or periglacial origin, including *Glacier-like formations* (GLF), *Concentric Crater Fill* (CCF), *Sublimation depressions*, *Thermal contraction polygons*, *Eroded crater walls*, *Older generation of CCF (?)* and *Mantle (?)*. The landforms have likely been formed and deformed during different climatic episodes of glaciation, where the recent glaciation probably occurred in the late Amazonian due to the sparse amount of impact craters in the study area.

Another aim of the study was to investigate the possibility that a warm-based glacier has been present in the study area. Observations such as the eroded crater walls and the degradation of the small crater's rim imply basal sliding and glacial abrasion may have occurred in the study area, which in turn suggests that a warm-based glacier may have existed. However, the formation of a warm-based glacier in the study area remains a mystery and further research, especially about the thermal environment and age of the craters, could contribute to understanding the geologic history of the study area.

References

Baker, D. M. H., Head, J. W., & Marchant, D. R. (2010). Flow patterns of lobate debris aprons and lineated valley fill north of Ismeniae Fossae, Mars; evidence for extensive mid-latitude glaciation in the late Amazonian. *Icarus (New York, N.Y. 1962),* 207(1), 186-209. https://doi.org/10.1016/j.icarus.2009.11.017

Benn, D. I., & Evans, D. J. A. (2014). *Glaciers and Glaciation (Second edition).* New York, Hodder Education. ISBN: 978-1-444-12839-0

Butcher, F. E. G., Balme, M. R., Gallagher, C., Arnold, N. S., Conway, S. J., Hagermann, A., & Lewis, S. R. (2017). Recent basal melting of a mid-latitude glacier on Mars. *Journal of geophysical research. Planets*, 122(12), 2445-2468. https://doi.org/10.1002/2017JE005434

Carr, M. H., & Head, J. W. (2010). Geologic history of Mars. *Earth and planetary science letters*, 294(3-4), 185-203. https://doi.org/10.1016/j.epsl.2009.06.042

Dickson, J. L., Head, J. W., & Marchant, D. R. (2008). Late Amazonian glaciation at the dichotomy boundary on Mars; evidence for glacial thickness maxima and multiple glacial phases. *Geology (Boulder)*, 36(5), 411-414. https://doi.org/10.1130/G24382A.1

Dickson, J. L., Head, J. W., & Fassett, C. I. (2012). Patterns of accumulation and flow of ice in the mid-latitudes of Mars during the Amazonian. *Icarus (New York, N.Y. 1962)*, 219(2), 723-732. https://doi.org/10.1016/j.icarus.2012.03.010

Forget, F., Costard, F., & Lognonné, P. (2007). *Planet Mars: Story of Another World*. Springer Praxis, Berlin, Heidelberg, New York. ISBN: 978-0-387-48925-4

Gallagher, C., Butcher, F. E. G., Balme, M., Smith, I., & Arnold, N. (2021). Landforms indicative of regional warm based glaciation, Phlegra Montes, Mars. *Icarus (New York, N.Y. 1962)*, 355, 114173. https://doi.org/10.1016/j.icarus.2020.114173

Hauber, E., Reiss, D., Preusker, F., Trauthan, F., Zanetti, M., Hiesinger, H., Jaumann, R., Johansson, L., Johnsson, A., van Gasselt, S., & Olvmo, M. (2011). Landscape evolution in Martian mid-latitude regions: Insights from analogous periglacial landforms in Svalbard. *Geological Society, London, Special Publications, 2011*, Vol. 356, pp. 111-.131, 356, 111-131.

Head, J. W., Mustard, J. F., Kreslavsky, M. A., Milliken, R. E., & Marchant, D. R. (2003). Recent ice ages on Mars. *Nature*, 426(6968), 797-802. https://doi.org/10.1038/nature02114

Hubbard, B., Souness, C., & Brough, S. (2014). Glacier-like forms on Mars. *The cryosphere*, 8(6), 2047-2061. https://doi.org/10.5194/tc-8-2047-2014

Laskar, J., Correia, A. C. M., Gastineau, M., Joutel, F., Levrard, B., & Robutel, P. (2004). Long term evolution and chaotic diffusion of the insolation quantities of Mars. *Icarus (New York, N.Y. 1962)*, 170(2), 343-364. https://doi.org/10.1016/j.icarus.2004.04.005

Levy, J. S., Fassett, C. I., Holt, J. W., Parsons, R., Cipolli, W., Goudge, T. A., Tebolt, M., Kuentz, L., Johnson, J., Ishraque, F., Cvijanovich, B., & Armstrong, I. (2021). Surface boulder banding indicates Martian debris-covered glaciers formed over multiple glaciations. *Proceedings of the National Academy of Sciences – PNAS*, 118(4). https://doi.org/10.1073/pnas.2015971118

Levy, J. S., Head, J. W., & Marchant, D. R. (2007). Lineated valley fill and lobate debris apron stratigraphy in Nilosyrtis Mensae, Mars: Evidence for phases of glacial modification of the dichotomy boundary. *Journal of Geophysical Research - Planets*, 112(E8), E08004-n/a. https://doi.org/10.1029/2006JE002852

Madeleine, J. B., Forget, F., Head, J.W., Levrard, B., Montmessin, F., & Millour, E. (2009). Amazonian northern mid-latitude glaciation on Mars: A proposed climate scenario. *Icarus (New York, N.Y. 1962)*, 203(2), 390-405. https://doi.org/10.1016/j.icarus.2009.04.037

Marchant, D. R., & Head, J. W. (2007). Antarctic dry valleys; microclimate zonation, variable geomorphic processes, and implications for assessing climate change on Mars. *Icarus* (New York, N.Y. 1962), 192(1), 187-222. https://doi.org/10.1016/j.icarus.2007.06.018

Mars Orbital Data Explorer (n.d.) PDS Geosciences Node. Washington University, St. Louis. Retrieved 2023-04-12 from: https://ode.rsl.wustl.edu/mars/index.aspx

Milliken, R. E., Mustard, J. F., & Goldsby, D. J. (2003). Viscous flow features on the surface of Mars; observations from high-resolution Mars Orbiter Camera (MOC) images. *Journal of Geophysical Research*, 108(E6), 5057-n/a. https://doi.org/10.1029/2002JE002005

Séjourné, A., Costard, F., Gargani, J., Soare, R. J., Fedorov, A., & Marmo, C. (2011). Scalloped depressions and small-sized polygons in western Utopia Planitia, Mars: A new formation hypothesis. *Planetary and space science*, 59(5), 412-422. https://doi.org/10.1016/j.pss.2011.01.007

The Bruce Murray Laboratory for Planetary Visualization (n.d.) The Murray Lab. California Institute of Technology. NASA/JPL/MSSS. Retrieved 2023-05-02 from: http://murray-lab.caltech.edu/CTX/

Woodley, S. Z., Butcher, F. E. G., Fawdon, P., Clark, C. D., Ng, F. S. L., Davis, J. M., & Gallagher, C. (2022). Multiple sites of recent wet-based glaciation identified from eskers in western Tempe Terra, Mars. *Icarus (New York, N.Y. 1962)*, 386, 115147. https://doi.org/10.1016/j.icarus.2022.115147
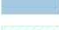
Appendix

Image of the study area and the geomorphological map.
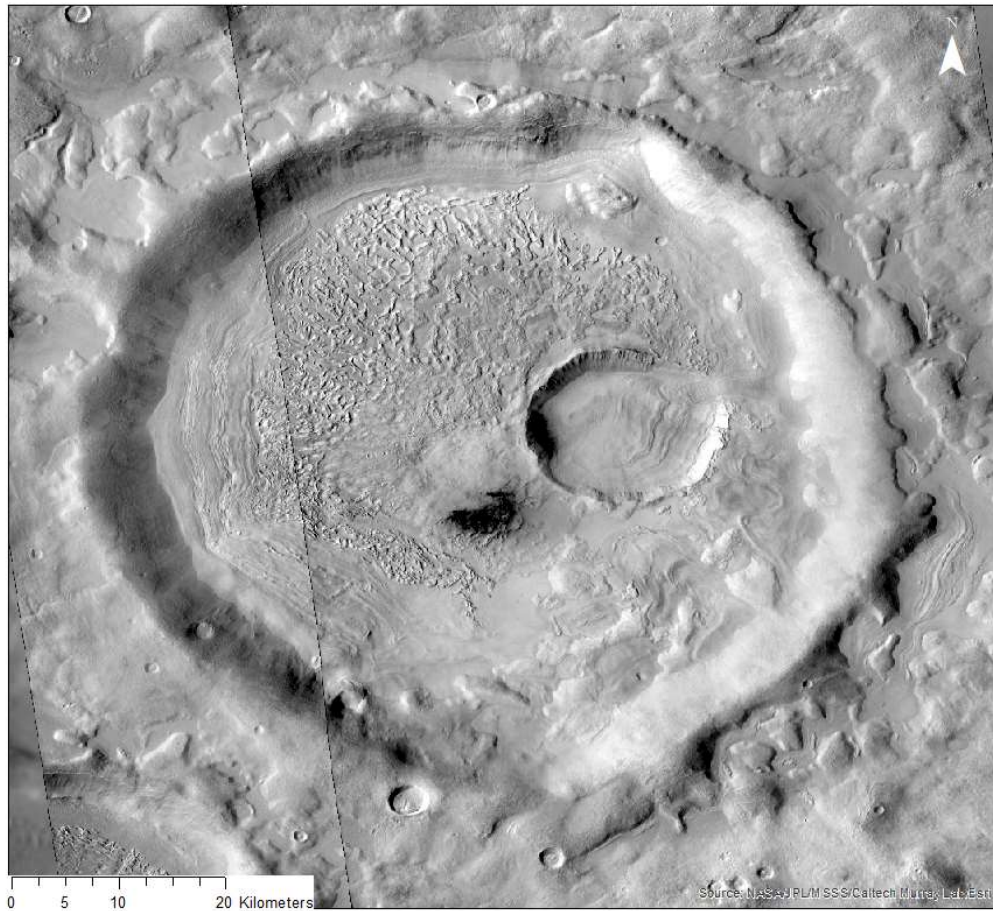
Geomorphological map of the study area

Landforms

- Craters
- Aeolian ripples
- Basaltic sand
- Scalloped depressions
- Craterwall
- Eroded Craterwall
- Glacier-Like Formation (GLF)
- Contraction polygons
- Concentric Crater Fill (CCF)
- Older generation of CCF (?)
- Mantle (?)
- Bedrock (?)

Source: NASA/JPL/MSSS/Caltech Murray Lab Esri

Cartographer: Aili Vesmes, 2023